Journal of Applied Polymer Science

Viscoelastic properties of borax loaded CMC-*g*-*cl*-poly(AAm) hydrogel composites and their boron nutrient release behavior

Dhruba Jyoti Sarkar,[1] Anupama Singh,[1] Shalini Rudra Gaur,[2] Aroon V Shenoy[3]

[1]Division of Agricultural Chemicals, ICAR-Indian Agricultural Research Institute, New Delhi, India

[2]Division of Food Science and Post Harvest Technology, ICAR-Indian Agricultural Research Institute, New Delhi, India

[3]SAICO- Technical Consultancy, Arlington Virginia

Correspondence to: A. Singh (E-mail: anupama.chikara@gmail.com)

ABSTRACT: Borax ($Na_2B_4O_7$, 10.5% Boron) loaded CMC-*g*-*cl*-poly(AAm) hydrogel composites were prepared by *in situ* grafting of acrylamide on to sodium carboxymethyl cellulose in the presence of borax by free radical polymerization technique to develop slow boron (B) delivery device. The composition, morphology, and mechanical properties of synthesized composites were studied by X-ray diffraction, Fourier transform infrared spectroscopy, scanning electron microscopy, texture analyser, and dynamic shear rheometer. Characterization revealed formation of borate ion (BO_3^{3-}) from borax during polymerization reaction leading to extensive crosslinking of cellulosic chains and generation of mechanically strong composite hydrogels. Dynamic release of BO_3^{3-} from the synthesized composites hydrogels followed Fickian diffusion mechanism and composites with high mechanical strength resulted in slow release of B. © 2016 Wiley Periodicals, Inc. J. Appl. Polym. Sci. **2016**, *133*, 43969.

KEYWORDS: composites; gels; kinetics; rheology

Received 24 November 2015; accepted 22 May 2016

DOI: 10.1002/app.43969

INTRODUCTION

In the present era of extensive agricultural practice, micronutrients are critical inputs in realizing high agricultural productivity, but their low use efficiencies are current cause of concern. To address such issues, in our earlier work we reported novel slow release zinc (Zn^{2+}) formulations using hydrogel composites as carriers.[1] Hydrogels and hydrogel composites are now finding considerable attention in the field of agriculture due to their unique water absorption and retention-release properties.[2–5] They have been reported effective in improving hydrophysical properties of soil and as carriers for controlled release of agrochemicals.[6–10] More recently they are extensively reported as carrier for fertilizer formulations including macro and micronutrients.[11–14] Although plant nutrients (N, P, K, and micronutrients) fertilizer formulations based on hydrogels are well reported, but their loading on viscoelastic properties of hydrogel carrier and release mechanism is hitherto unknown.

In the present work, we report synthesis of borax (10.5% B) loaded CMC-*g*-*cl*-poly(AAm) hydrogel composites as slow B delivery device and the effect of different synthesis parameters on the viscoelastic properties and release behavior of B. Borax is used in agriculture as a source of B, an important micronutrient for crop health and its deficiency in soil is an important problem and realized all over the world.[15–18] Application rates of borax are high at 2–5 kg/hectare and its use efficiency remains very low due to losses from light textured acidic soil receiving high precipitation, red lateritic soil, calcareous soil, and soil with low organic matter.[17] In polymer chemistry, borax was reported as a crosslinker for polysaccharide chains containing hydroxyl groups and borax loaded composites were reported with improve mechanical, thermal, chemical resistance, and barrier properties.[19–21] For example, barrier properties of poly(vinyl alcohol)-graphene oxide composite film was improved by borax crosslinking.[21] Borate orthoester covalent bonding between graphene oxide nanosheets were reported to be one of the stiffest materials.[22] Moreover loading of polymer with borax has been found to improve the intercalation or exfoliation morphology of clay hybrid biocomposite as well as mechanical properties of crosslinked polymer.[23,24] Other than borax, introduction of nanoclay,[25] double network structures,[26] polyampholytes,[27] temperature induced nonswellability,[28] and so forth. have also been reported recently to improve the mechanical strength of hydrogel by altering their viscoelastic and physical properties. The present work aims at revealing viscoelastic changes of CMC-*g*-*cl*-poly(AAm) hydrogels when loaded with borax as a source of micronutrient (B) and their effect on B release pattern. This type of information would be useful in developing agriculturally suitable hydrogel-based nutrient formulation for integrated water and nutrient management of industrial crops.

EXPERIMENTAL

Chemicals

Sodium carboxymethyl cellulose (NaCMC) (viscosity range 1100-1900cps), acrylamide (AM), *N*,*N*-methylene bisacrylamide (MBA), ammonium peroxodisulphate (APS) were procured from Merck Specialties Pvt. Ltd., Mumbai, India and used as received without further purification. Borax ($Na_2BO_4O_7$. $10H_2O$) was purchased from Thermo Fisher Scientific India Pvt. Ltd., Mumbai, India.

Preparation of Borax Loaded CMC-*g*-*cl*-Poly(AAm) Composites

The borax loaded CMC-g-cl-poly(AAm) composites (BSAPCs) were synthesized by *in situ* grafting of AM on the NaCMC backbone in the presence of MBA, APS, and borax by free radical polymerization technique reported previously.[1] The typical procedure used was as follows: Weighed quantities of AM and MBA were dissolved in distilled water. A mixture of NaCMC and borax was added to the solution with continuous mechanical stirring till a homogenous mixture (feed mass) is formed. The polymerization was initiated by addition of APS. The feed mass was kept at 80 °C till gel point was attained. The cross-linked gel mass was oven dried at 70 °C till constant weight. The grafting yield (G_y) and grafting efficiency (G_e), to characterize the composites synthesis process were calculated by the following equations[29]:

$$G_y = (W_{BSAPCx} - W_{NaCMC}) / W_{NaCMC} \quad (1)$$

$$G_e = (W_{BSAPCx} - W_{NaCMC}) / (W_{BSAPC} - W_{NaCMC}) \quad (2)$$

Here, W_{NaCMC}, W_{BSAPC}, and W_{BSAPCx} are the weight of NaCMC, BSAPC before and after extraction of homopolymer, respectively. AM homopolymer was removed by Soxhlet extraction with a 60:40 (V/V) mixture of ethylene glycol and acetic acid for 2 h.[30]

Characterization

Prepared composites were characterized by wide angle X-ray diffraction (XRD) using Philips PW1710 diffractometer equipped with Philips PW1728 X-ray generator. The scanning range and scanning rate were kept at 1–50° 2θ and 1.2° 2θ min^{-1}, respectively. The functional group transformation were analyzed using Bruker Fourier Transform Infrared Spectrophotometer (FT-IR) (Model Alpha ATR & Bruker, KBR pelleting method) under dry air at room temperature.Scanning electron microscopy (SEM) images were obtained using ZEISS EVO MA10, 20kV, and 10 pa after 30 nm palladium coating.

Tensile strength of representative BSAPCs was assessed using a TA.XT2i® Texture Analyzer (Stable Micro Systems Ltd., Godalming, Surrey, U.K.) programmed with the Texture Exponent software. The samples were cut into uniform strips 3 × 5.0 cm. A probe labeled Tensile Grips (A/TG) was used to extend each sample until it breaks.

The rheological properties of equilibrated swollen BSAPCs were measured using an dynamic shear rheometer (MCR-52, Anton Paar, Germany), fitted with cone and plate measuring system (50-mm diameter) at 25 °C with a gap of 0.1 mm between the plates. An equilibration time of 5 min was provided for hydrogel composite to attain measurement temperature after placing sample between the cone and plate assembly. To determine gel points of representative BSAPCs, temperature sweep tests were conducted with linear temperature change from 30 to 100 °C at a rate of 2 °C min^{-1}, at constant strain (0.1%) and frequency (50 rad s^{-1}). For dynamic rheological tests, linear viscoelastic region (LVR) was established by conducting a strain test in the range of 0.1 to 100% at constant frequency of 10 rad s^{-1}. Following this, frequency sweep tests (frequency: 0.1 to 100 rad s^{-1}) in logarithmic progression were performed in a controlled strain mode at constant strain of 0.1%, which lay well within the LVR for all the studied hydrogels.

Swelling Investigation

Accurately weighed powdered BSAPCs (0.1 g, particle size < 63 μm) were taken in nylon bags and immersed in excess of distilled water (100 mL) (pH 7.0, EC 0.001 Mhos cm^{-1}) and kept at constant temperature (30 °C) until equilibration was attained. The equilibrated swollen BSAPCs were allowed to drain for 10 min to remove free water from nylon bags. Each bag was weighed to determine the weight of the swollen BSAPCs. The water absorption capacity (Q_{H_2O}, g/g, dry weight basis) was calculated using the equation:

$$Q_{H_2O} = (W_e - W_x) / W_x \quad (3)$$

Here, W_x is the weight of xerogel or BSAPCs in glassy state and W_e is the weight of swollen BSAPCs at equilibration.

Determination of B Loading Efficiency

Di-acid digestion method[31] was used to estimate the amount of B loaded in the matrices of BSAPCs. Briefly, accurately weighed developed composites (0.1 g, particle size 100–240 mesh) were taken in conical flasks was treated with 10 mL of concentrated nitric acid (HNO_3) and kept under fume hood for overnight. After 12 h reaction mass was treated with di-acid mixture (HNO_3:$HCLO_3$: 3:1, 12 mL) and further heated at 200 °C for 4–6 h till the disappearance of brown color. The content of the flask was filtered and volume made up to 100 ml. Estimation of B in the sample was done by Azomethine-H method.[32] Briefly, 1 mL of the sample filtrate was taken in 10–15 mL polypropylene tube, on which 2 mL buffer solution (Ammonium acetate: EDTA: Acetic acid) and 2 mL Azomethine-H reagent (Azomethine-H: L-ascorbic acid) was added. Azomethine-H forms a stable colored complex with B at pH 5.1 in aqueous media and the color intensity was measured in UV-VIS to know the concentration of B. Loading efficiency of the B (BLC, %) was calculated as follows:

$$\text{BLC}\,(\%) = (\text{B detected in BSAPCs} / \text{B introduced in BSAPCs}) \times 100 \quad (4)$$

Release of BO_3^{3-} from BSAPCs

As plant absorbs B in the form of H_3BO_3, the effect of reactants namely borax, MBA, and AM content in the feed mass on release pattern of BO_3^{3-} from BSAPCs matrix was assessed by tea bag method as reported previously.[1,16] Briefly a dry powdered BSAPC specimen (0.1 g, particle size 80 mesh) taken in nylon sachet (3cm × 3 cm; 200 mesh) was immersed in distilled water (100 mL) and incubated at room temperature (30 ± 2 °C). On *n*th day 1 mL aliquot was analyzed by Azomethine-H method for BO_3^{3-} estimation.[1,32]

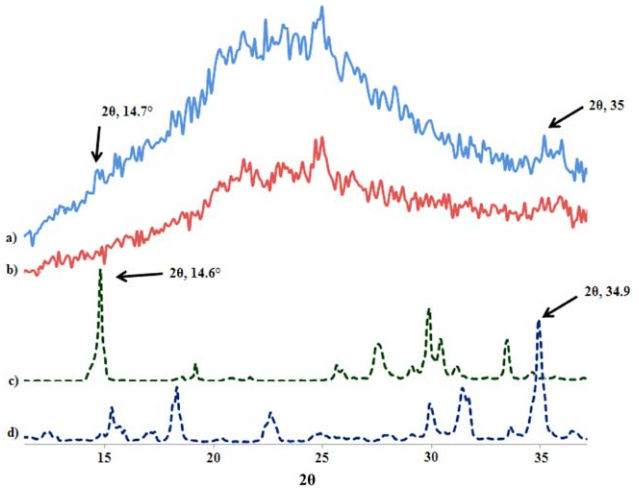

Figure 1. XRD of (a) BSAPC-E3 [CMC-*g*-*cl*-poly(AAm) loaded with 3.64% B]; (b) SAPC [CMC-*g*-*cl*-poly(AAm)]; (c) Boric acid (H3BO3); and (d) Borax (Na2BO4O7. 10H2O). [Color figure can be viewed in the online issue, which is available at wileyonlinelibrary.com.]

Korsmeyer–Peppas equation[33] was used to describe the mechanism of BO_3^{3-} release from BKSAPCs. Release data were analyzed by the following equation:

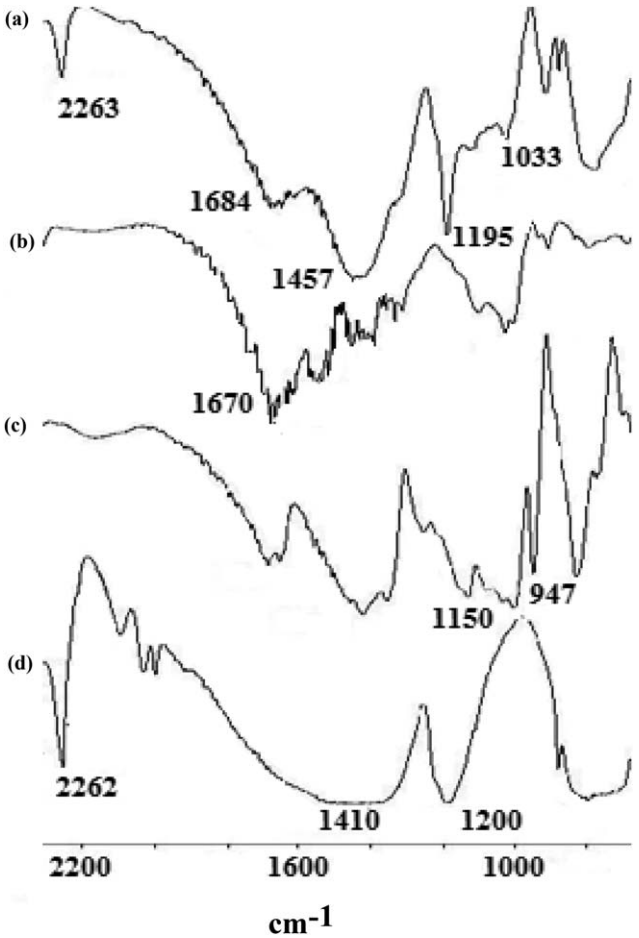

Figure 2. FTIR spectra of (a) BSAPC-E3 [CMC-*g*-*cl*-poly(AAm) loaded with 3.64% B]; (b) SAPC [CMC-*g*-*cl*-poly(AAm)]; (c) Borax (Na2BO4O7. 10H2O); and (d) Boric acid (H3BO3).

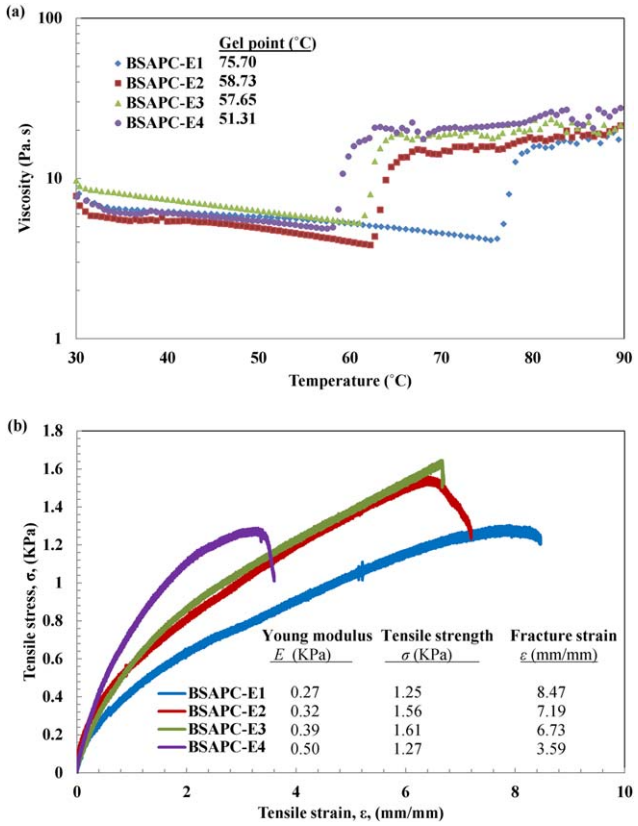

Figure 3. (a) Gel point analysis and (b) stress-strain curves of representative BSAPCs. (BSAPC-E1, 11.6% borax; BSAPC-E2, 16.5% borax; BSAPC-E3 20.8% borax; BSAPC-E4, 28.3% borax). [Color figure can be viewed in the online issue, which is available at wileyonlinelibrary.com.]

$$\frac{M_t}{M_o} = at^b \tag{5}$$

Here, M_t is the BO_3^{3-} form of B released at time t; M_o is the total B content of BSAPCs; *a*, kinetic constant, and *b*, the diffusion exponent that predicts the release mechanism. For hydrogels, when $b \leq 0.5$, the mechanism is Fickian diffusion.[33] When $b = 1$, Case II transport occurs, leading to zero-order release. When the value of *b* is between 0.5 and 1, anomalous transport is observed.

RESULTS AND DISCUSSION

Characterization of BSAPC

Figure 1 shows XRD patterns of a representative BSAPC (BSAPC-E3), SAPC [CMC-*g*-*cl*-Poly(AAm)], borax, and boric acid. BSAPC-E3 showed diffraction peak at 2θ, 35°, corresponding to the peak of pure borax (2θ, 34.9°) indicating successful loading of borax in composite matrix. XRD spectrum of BSAPC also showed a small peak at 2θ, 14.6° corresponding to boric acid (2θ, 14.9°) revealing formation of borate ion from borax ($B_4O_7^{2-} \rightarrow BO_3^{3-}$) during present composite synthesis.[34] This observation was substantiated by the presence of characteristic FT-IR bands of boric acid (asymmetric B—O stretching at 1310–1400 cm^{-1} and in-plane B—O—H bending at 1200 cm^{-1}) and borax (asymmetric B—O stretching band at 947 cm^{-1} and in-plane B—O—H bending at 1150 cm^{-1})[35] in the

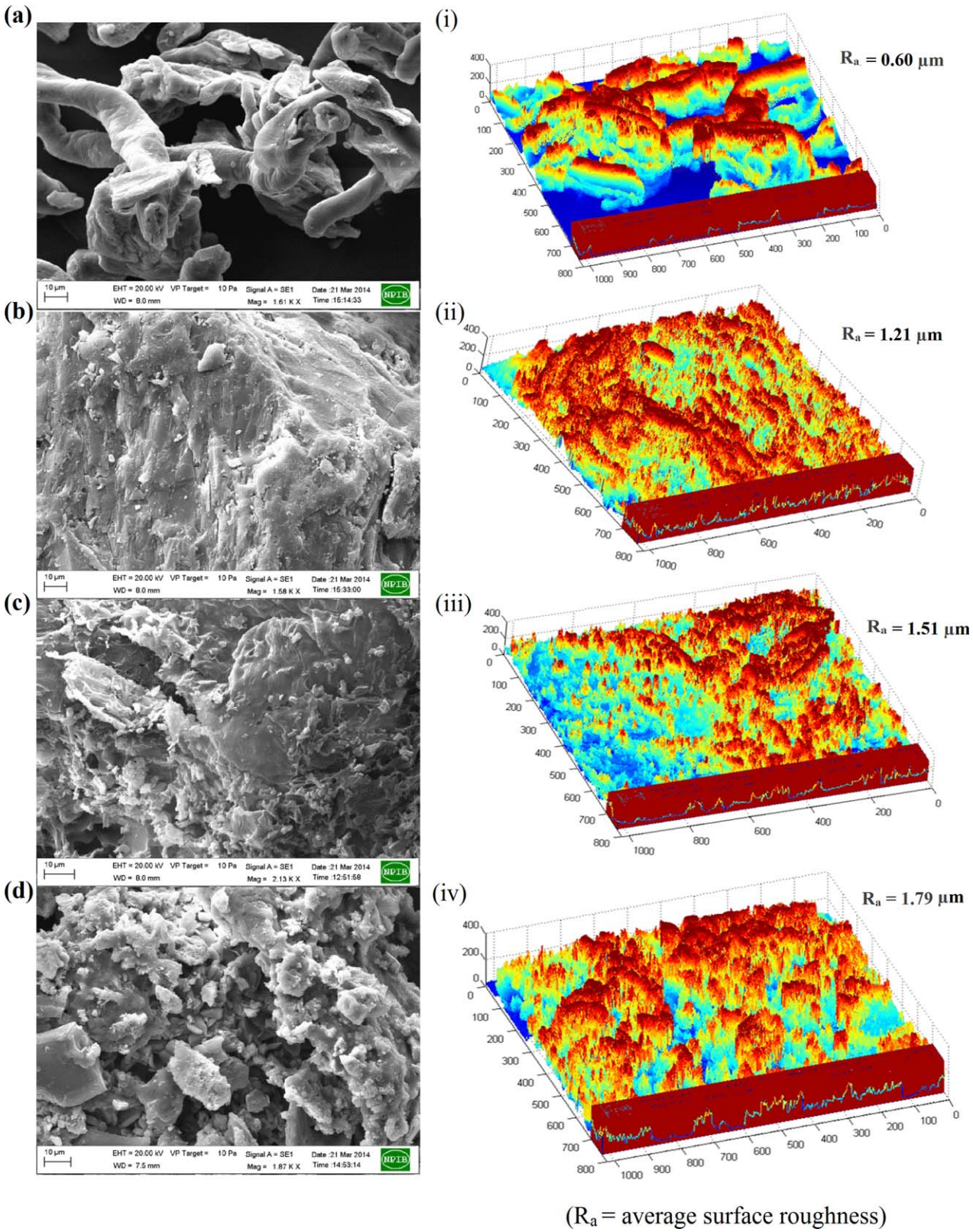

Figure 4. Scanning electron micrographs and corresponding 3-D mesh diagrams of NaCMC (a,i); SAPC containing 0.0% B (b,ii); BSAPC-E1 containing 2.03% B (c,iii); BSAPC-E4 containing 4.95% B (d,iv). [Color figure can be viewed in the online issue, which is available at wileyonlinelibrary.com.]

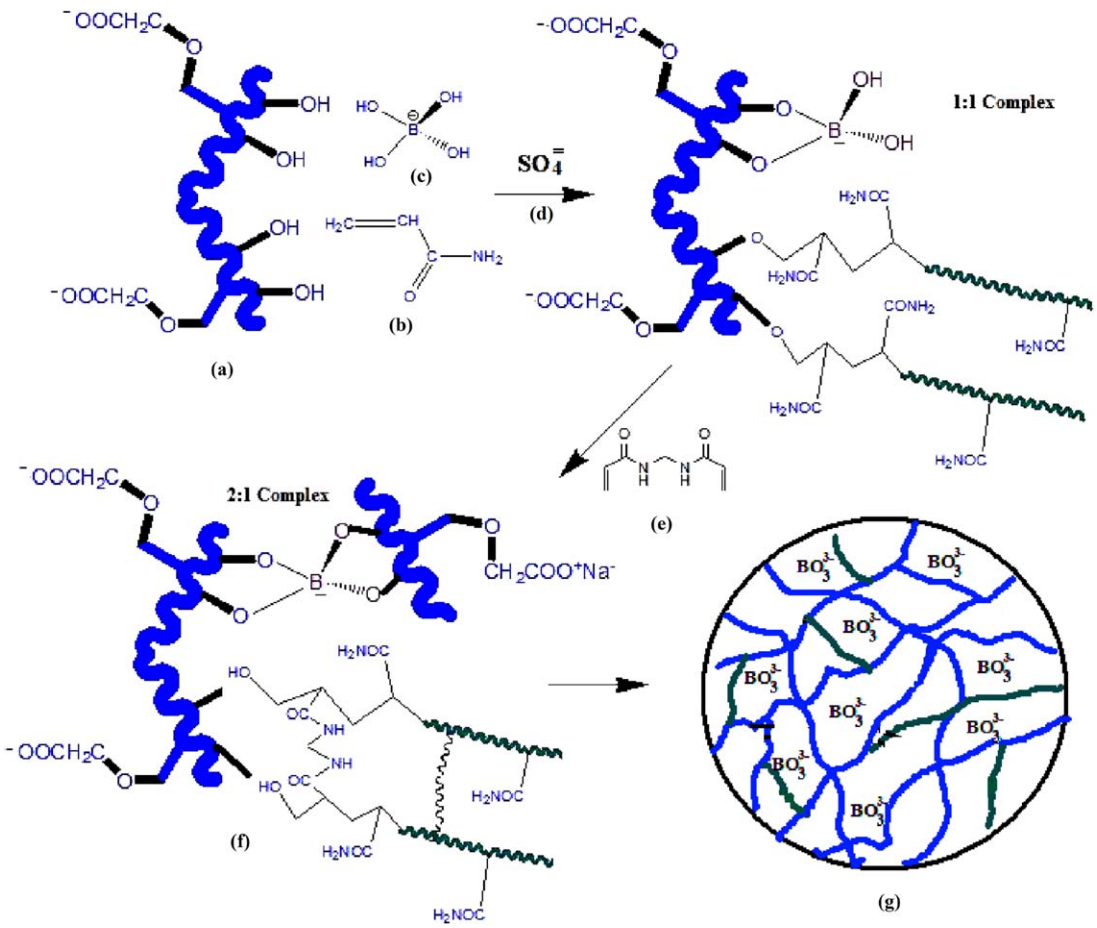

Figure 5. Schematic diagram of composites synthesis (a) Sodium carboxymethyl cellulose (NaCMC); (b) Acrylamide (AM); (c) borate ion (BO_3^{3-}); (d) Ammonium peroxodisulphate (APS); (e) *N,N*-methylene bisacrylamide (MBA); and (f,g) borax loaded CMC-*g*-*cl*-poly(AAm) (BSAPC). [Color figure can be viewed in the online issue, which is available at wileyonlinelibrary.com.]

FT-IR spectrum of BSAPC-E3 (Figure 2). These bands were absent in FT-IR spectrum of corresponding SAPC [Figure 2(b)]. Characterization through XRD and FT-IR established (i) successful loading of borax in the composite matrix of BSAPCs and (ii) formation of BO_3^{3-} may be through partial *in situ* hydrolysis of borax.[34]

The temperature sweep tests in rheometer showed significant influence of borax loading on onset of gel point temperatures of representative BSAPCs. At 70 °C, BSAPC-E1 remained in liquid form and on heating to 75.70 °C gelation was observed [Figure 3(a)]. A steep increase in viscosity indicates that the feed mass molecules of composites start to rearrange and by crosslinking gel is formed. High content of borax in the feed mass of BSAPCs led to lowering of gel point temperature. Gelation temperature of representative BSAPCs followed the order: BSAPC-E1, 75.70 °C > BSAPC-E2, 58.73 °C > BSAPC-E3, 57.65 °C > BSAPC-E4, 51.31 °C. This variation of gel point with more borax content in BSAPCs can be explained by higher availability of BO_3^{3-} for crosslinking of polysaccharide chain of composites.

Figure 3(b) shows stress–strain curve of representative BSAPCs with different borax contents. Young's modulus, *E*, Tensile strength (ultimate stress), σ, and Fracture strain (ultimate strain), ε; of the representative hydrogel composites were highly dependent on the borax content. Incorporation of higher amount of borax in BSAPCs resulted in a mechanically tougher composites, indicated by higher *E* values (0.50 KPa, BSAPC-E4 versus 0.27 KPa, BSAPC-E1) and higher σ values till borax content of 20.8% (1.61 KPa, BSAPC-E3 versus 1.25 KPa, BSAPC-E1), and lower ϵ values (3.59 mm/mm, BSAPC-E4 versus 8.47 mm/mm, BSAPC-E1) as the borax content in the feed mass increased from 11.6 to 28.3%.[36]

Figure 4 shows SEM and corresponding 3D mesh diagram of NaCMC, SAPC, and BSAPCs (BSAPC-E1 and BSAPC-E4). SEM images were subjected to digital image processing using image processing toolbox of MATLAB (R2011a) which can efficiently convert the SEM images to *n* by *m* 3D matrix from. The average surface roughness (R_a) was calculated to differentiate surface morphologies of samples.[37]

$$R_a = \frac{1}{n}\sum_{i=1}^{n} |y_i| \tag{6}$$

Here y_i is the distance from the average height of a profile (the mean line) for measurement *i*, and *n* is the number of measurements. Three-dimensioanl mesh diagram of indicates that due to borax loading roughness of the composite surface (R_a) was

Table I. Effect of Synthesis Parameters on Graft Yield and Graft Efficiency of BSAPCs

	Synthesis parameters				
BSAPCs	AM: NaCMC	MBA (ppm)	Borax (%)	G_e[a]	G_y[b]
E1	2.5:1.0	748.5	11.6	0.88^{b}	2.67^{E}
E2	2.5:1.0	748.5	16.5	0.82^{CD}	2.73^{DE}
E3	2.5:1.0	748.5	20.8	0.75^{EF}	2.83^{DE}
E4	2.5:1.0	748.5	28.3	0.73^{F}	2.93^{CDE}
D1	2.5:1.0	187.2	4.99	0.43^{G}	0.71^{G}
D2	2.5:1.0	249.6	4.99	0.48^{G}	0.98^{G}
D3	2.5:1.0	499.2	4.99	0.78^{DE}	2.08^{F}
D4	2.5:1.0	1246.9	4.99	0.73^{EF}	2.05^{F}
C1	3.0:1.0	748.5	4.99	0.98^{a}	3.14^{bCD}
C2	3.5:1.0	748.5	4.99	0.87^{bC}	3.31^{bC}
C3	4.0:1.0	748.5	4.99	0.83^{CD}	3.54^{b}
C4	5.0:1.0	748.5	4.99	0.81^{D}	5.09^{a}
P-value				<0.0001	<0.0001
CV(%)				1.96	4.39
Tukey HSD at 1%				0.0529	0.4188

Synthesis parameters: Initiator (wt %): 3.0, V_{H2O} (mL) = 20.
[a] Grafting efficiency (g/g).
[b] Grafting yield (g/g).
Means with at least one letter common are not statistically significant (1%) using TUKEY's Honest Significant Difference (HSD); CV (%), coefficient of variation.

enhanced. The probable mechanism of BSAPC synthesis in schematic diagram is shown in Figure 5.

Graft Yield and Grafting Efficiency

The effect of synthesis parameters namely crosslinker (MBA), monomer-backbone ratio (AM:NaCMC), and borax content on graft yield (G_y) and grafting efficiency (G_e) is shown in Table I. Higher content of MBA in the composite matrix (BSAPCs) resulted higher G_y and G_e, due to generation of more crosslinked polyacrylamide chain [poly(AAm)] grafted per unit of NaCMC backbone. Similarly, higher content of AM in BSAPCs resulted increase in G_y although composites with AM:NaCMC ratio above 3.0:1 showed low G_e which may be due to higher radical formation on AM leading to lowering of viscosity of polymerization medium and increase rate of termination process.[38] Increase amount of borax in BSAPCs resulted higher G_y, due to generation of more borate crosslinked point in the cellulosic chain of NaCMC leading to formation of higher amount of net crosslinked polymeric material[20,21] and lower G_e which may be resulted from low availability of grafting sites of NaCMC per unit of AM.

Effect of Synthesis Parameters on Viscoelastic and Water Absorbency Properties of BSAPCs

Variation of storage modulus (G') with frequency (ω) provides the "mechanical spectrum" of a material.[39] Mechanical spectrum of BSAPCs as a function of different synthesis parameters is shown in Figure 6. Correlation between storage modulus (G') and frequency (ω) is expressed by the following rheological model[40,41]:

$$G' = \frac{K}{m'} - (1-n')\omega^{n'}\left(1+\omega^2\right)^{\frac{n'-n''}{2}}\left[1+\frac{(n''-n')\ \omega^2}{(1+n')(1+\omega^2)}\right] \quad (7)$$

Here, K is the complex viscosity at frequency of 1 radian s^{-1} and at $n' = n''$, n' and n'' are the slope of the $|\eta^*|$ versus ω curve in the region of $0.1 \le \omega \le 1$ and $0.1 \le \omega \le 10^2$, respectively. m' is an adjustable parameter. The above equation was chosen because it was observed that the complex viscosity curves in Figure 6 showed two distinct straight line regions in the low and high frequency regimes. A high value of K and a low value of n' and n'' indicate hydrogels with higher mechanical strength which implies that greater force or energy is required to make the hydrogel flow.[40,41] The degree of ω dependence of G' can also be determined by the well-known "Power-Law" parameters.[42]

$$G' = A\ \omega^B \quad (8)$$

Here A is the intercept and the exponent B is the slope of log–log plot of G' versus ω. The slope B is related to the material strength factor of the gel and a lower value of B indicates gel of higher mechanical strength.

Over the test frequency range (ω), storage modulus (G') of BSAPCs increased with increase in boron content (2.03 to 4.95%) [Figure 6(a)]. Similar behavior has been previously reported in borax crosslinked scleroglucan hydrogels.[43] The test rheological models [eq. (7) and (8)] quantified the influence of different synthesis parameters on the viscoelastic properties of BSAPCs. Among them eq. (7) was chosen the as best fit model with a high coefficient of determination (R^2). Log–log plot of $|\eta^*|$ versus ω curve (Figure 6) of BSAPCs showed two distinct

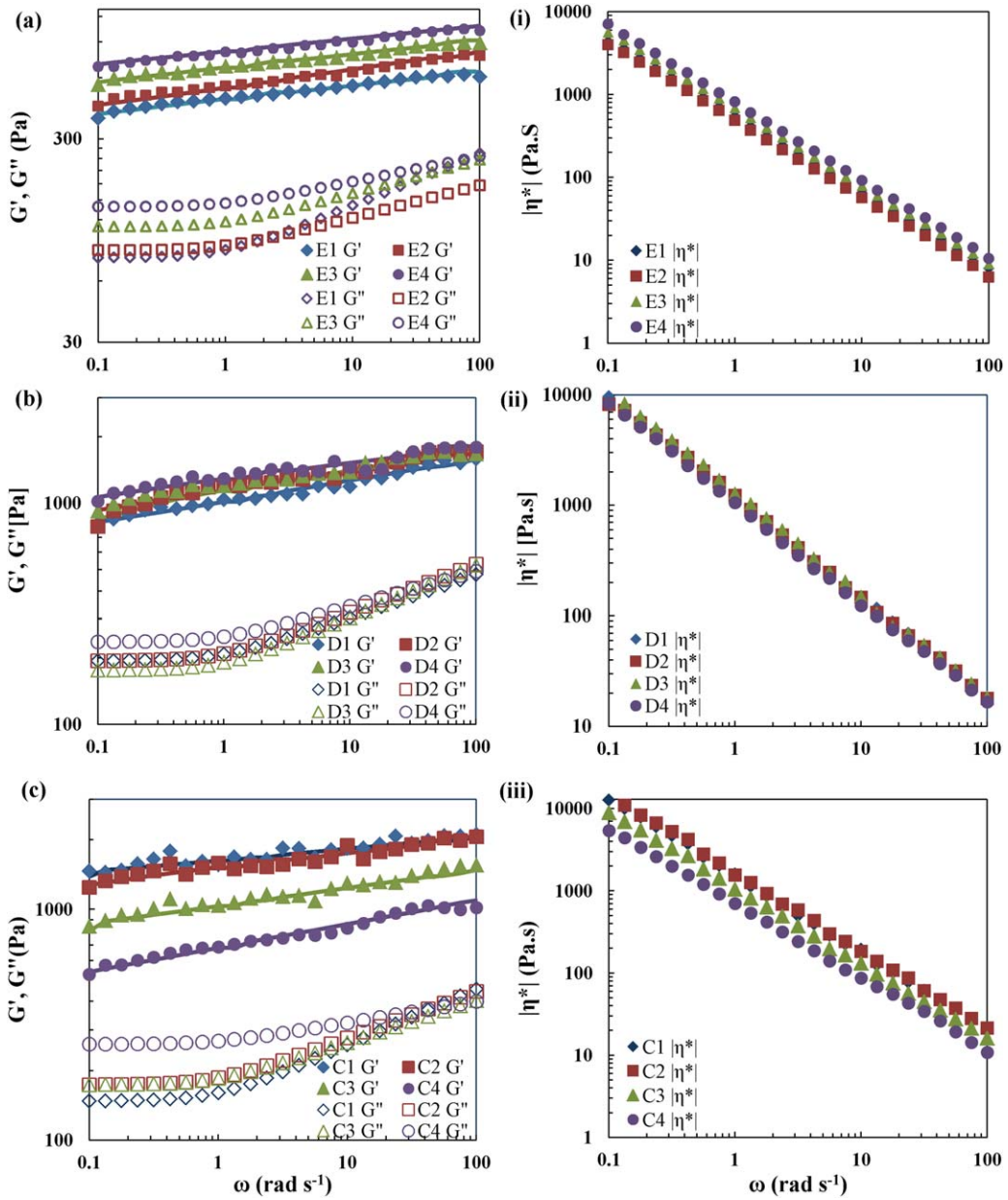

Figure 6. Storage modulus (G') and loss modulus (G'') versus angular frequency (ω) curves of BSAPCs at 25 °C with varied content of (a) borax, (b) MBA and (c) AM. Solid lines in G' versus ω curves indicate that theoretical model [eq. (7)] fits through experimental data points. [Color figure can be viewed in the online issue, which is available at wileyonlinelibrary.com.]

slopes (n' and n'') in the low ($0.1 \leq \omega \leq 1$) and high frequency ($1 \leq \omega \leq 10^2$) regions. In both low and high-frequency regions, there was a decrease of slope values (n' and n'') with an increase of borax loading in BSAPCs (Table II) which indicates an improvement of "solid like" properties of BSAPCs due to the higher loading of borax inside the matrix. This fact can be explained by higher crosslinking of cellulosic chains of NaCMC by BO_3^{3-}, formed during synthesis of BSAPCs (Figure 5). Borate crosslinking of cellulosic chains of NaCMC has restricted molecular mobility and reduction of free volume, implied increase of complex viscosities BSAPCs. The complex viscosities of E1, E2, E3, and E4 at ω of 1 radian s^{-1} followed the order: E1 (482.00) < E2 (550.00) < E3 (691.00) < E4 (814.00). Table II also depicts that, the increase of borax content in BSAPCs had led to an increase of A value and reduction of B value of the "Power-Law" ($G' = A\ \omega^B$). The value of B (slope) for the E2 (2.88% B) was higher (0.077) than the E4 (4.95% B) (0.062) indicating that the E2 was weaker gel system than E4.

Higher crosslinker (MBA) content in BSAPCs led to high value of complex viscosity (K) (D1, 1210< D2, 1230 < D3, 1300 < D4,1410) at ω of 1 radian s^{-1} and reduction of n' value (D1, 0.095 = D2, 0.095 > D3, 0.090 > D4, 0.089) (Table II) . Similarly, B value of power equation (Table II) [eq. (8)] was

Table II. Effect of Synthesis Parameters on Viscoelastic properties, Crosslink Density, and Water Absorption Behavior of BSAPCs

	$G' = \frac{K}{m'} - (1-n')\omega^{n'}(1+\omega^2)^{\frac{n'-n''}{2}}\left[1+\frac{(n''-n')\ \omega^2}{(1+n')(1+\omega^2)}\right]$					$G' = A\omega^B$				
BKSAPCs	K	n'	n''	m'	R^2	A	B	R^2	CD[a]	Q_{H_2O}[b]
E1	482.00	0.080	0.090	0.952	0.996	471.35	0.065	0.980	0.191	51.33^{B}
E2	550.00	0.079	0.067	0.932	0.998	543.23	0.077	0.988	0.219	47.10^{C}
E3	691.00	0.074	0.067	0.945	0.998	673.76	0.064	0.988	0.275	47.21^{C}
E4	814.00	0.062	0.063	0.945	0.999	788.62	0.062	0.989	0.323	41.03^{D}
D1	1210.00	0.095	0.082	0.945	0.998	1019.60	0.092	0.976	0.419	52.86^{B}
D2	1230.00	0.095	0.096	0.858	0.996	1139.60	0.095	0.950	0.484	45.21^{C}
D3	1300.00	0.090	0.073	0.902	0.979	1199.30	0.082	0.966	0.488	40.65^{D}
D4	1410.00	0.089	0.096	0.956	0.993	1291.60	0.070	0.916	0.520	37.43^{DE}
C1	1570.00	0.043	0.051	0.930	0.990	1658.40	0.051	0.865	0.634	36.37^{E}
C2	1610.00	0.073	0.078	0.946	0.987	1520.10	0.062	0.912	0.642	37.37^{DE}
C3	1050.00	0.086	0.100	0.947	0.993	1062.90	0.078	0.946	0.419	48.06^{C}
C4	705.00	0.105	0.103	0.923	0.999	686.67	0.095	0.977	0.278	64.53^{A}
P-value										<0.0001
CV(%)										2.37
										3.9412

[a] CD, crosslink density ($\times 10^{-6}$ mole cm^{-3}).
[b] H_2O, water absorption capacity.
Means with at least one letter common are not statistically significant (1%) using TUKEY's Honest Significant Difference (HSD); CV (%), coefficient of variation.

reduced with the high content of MBA in BSAPCs. The *B* value of the D1 (187.2 ppm MBA) was higher (0.092) than D4 (1246.9 ppm MBA) (0.070) indicating that the D1 was weaker gel as compared to D4 which can be attributed to the generation of more crosslinked Poly(AAm). Monomer (AM) played an important role in influencing the mechanical strength of BSAPCs, observed by reduction of complex viscosity (K) and an increase of both n' and n'' with increase of AM: NaCMC ratio from 3.0: 1.0 (C1) to 5.0: 1.0 (C4) (Table II). This kind of behavior may be attributed to lowering of crosslink density with increase of monomeric unit per unit reaction mass when the amount of crosslinker is fixed. "Power-Law" slope parameter (B) also showed steady increment in value with the increase of AM:NaCMC ratio in the BSAPCs matrices.

Previously it was reported that the storage modulus (G') of polyacrylate hydrogels is directly related to the crosslink density and follows the equation[44]:

$$G' = \nu RT \tag{9}$$

Here, ν is the crosslink sites per unit volume of hydrogels; T is the temperature (K) and R is the gas constant (8.3145 m^3 Pa K^{-1} Mol^{-1}). The above equation was used to calculate the crosslink densities of developed BSAPCs and is shown in Table II. In the present study, lower crosslink density of BSAPCs was observed with increase in AM content, which can be attributed to higher AM: MBA ratio in test matrix resulting development of loosely crosslinked polymeric network. BSAPCs with higher crosslink densities were observed with increase in amount of borax and MBA due to their crosslinking ability with cellulosic chain of NaCMC and AM, respectively. These changes of crosslink density due to varied synthesis parameters ultimately influenced the water absorbency (Q_{H_2O}) behavior of BSAPCs (Table II). Reduction of Q_{H_2O} value with increase of MBA and borax content was observed which is explained in terms of generation of extensive crosslink points, resulting highly crosslinked structures that cannot expand sufficiently to hold large quantities of water.[44] Higher crosslink density and the lower equilibrium swelling capacity (Q_{H_2O}) can be correlated with storage modulus (G'). Increase of G' of BSAPCs over test frequency (ω) range with increase in MBA and borax content may be attributed to the higher corsslinking density leading to higher mechanical strength of polymeric network with lower mobility of water inside the composite and poor macromolecular relaxation.[45] Q_{H_2O} values of BSAPCs prepared by taking AM: NaCMC ratio, 5:1 was maximum (Table I) whereas gel could not be produced with AM: NaCMC ratio < 3:1. This could be formed due to increase in homopolymer percentage.[46] Reduction of polymeric strength (G') with increase of AM content can be attributed to introduction of more monomeric (AM) units in the polymeric chains leading to loosely crosslinked polymeric network.

Effect of Synthesis Parameter on BO_3^{3-} Release Behavior of BSAPCs

Periodic release of BO_3^{3-} from BSAPCs in water showed influence of reaction parameters on the release kinetics (Figure 7). Figure 7(a) depicts that BSAPCs with high B loading (Table III; E3, 3.64% B and E4, 4.59% B) showed slower BO_3^{3-} release

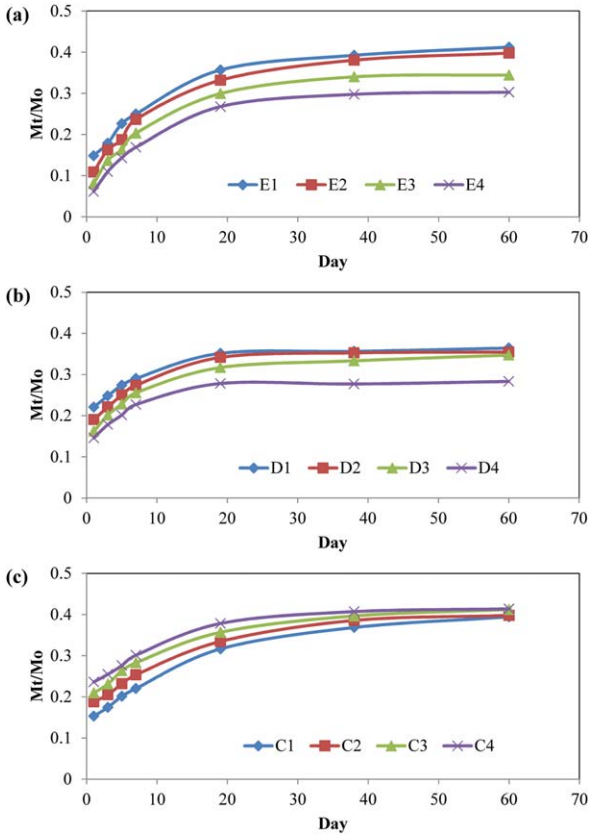

Figure 7. BO_3^{3-} release behavior of BSAPCs with varied content of (a) borax, (b) MBA, and (c) AM. [Color figure can be viewed in the online issue, which is available at wileyonlinelibrary.com.]

profile than corresponding lower B content. Rheological investigation of BSAPCs in present work has proven that higher borax content in reaction feed mass led to generation of extensively crosslinked polymer networks (Table II) which manifested itself in terms of slower release of BO_3^{3-} from E3 and E4.[47] On 60th day, E3 and E4 released about 28 to 34% of loaded B as compared to around 40% in case of E1 and E2. Similarly, BSAPCs with high MBA content showed slower release rate due to generation of more crosslinked Poly(AAm) in composite matrix [Figure 7(b)], although in the present study the effect of MBA content in lower test range (187.23 to 499.12 μg g^{-1} of feed mass) showed little effect on the release pattern of BO_3^{3-}. On 60th day, D4 released about 25% of initially loaded B as compared to 35% in case of D1, D2 and D3. Figure 7(c) shows that decrease in AM content resulted in slower BO_3^{3-} release during the initial period (1 to 10 days). Variation of AM content in BSAPCs on the cumulative release has resulted expected release pattern: C1 > C2 > C3 > C4.

Mechanism of BO_3^{3-} Release from BSAPCs

Increase of borax and MBA content and decrease of AM: NaCMC ratio in the feed mass of BSAPCs resulted in slower rate of BO_3^{3-} release from the matrix which in the present study is attributed to generation of more barrier properties induced by enhanced mechanical strength. The mechanism of BO_3^{3-} release from BSAPCs has been predicted using diffusion exponent (b) value obtained from Korsmeyer–Peppas equation [eq. (5)]. In the present study, the value b ranged from 0.13 to 0.34 (Table III) which indicates that the release mechanism followed Fickian diffusion and was not a function of degree of swelling.[33]

Table III. Boron (B) Loading Efficiency, Release Kinetics Parameters, and Diffusion Coefficient of BO_3^{3-} from BSAPCs

			$M_t/M_o = at^b$			
BSAPCs	B[a]	BLC[b]	a	b	R	D_i[c]
E1	2.03	91.09 ± 1.72	0.15^{FG}	0.26^{C}	0.98	3.46
E2	2.88	94.25 ± 4.08	0.12^{HI}	0.30^{B}	0.98	2.21
E3	3.64	89.69 ± 3.69	0.11^{I}	0.31^{B}	0.97	1.86
E4	4.95	63.23 ± 2.98	0.08^{J}	0.34^{A}	0.97	0.98
D1	0.87	90.92 ± 1.09	0.23^{A}	0.13^{H}	0.97	8.13
D2	0.87	85.25 ± 2.59	0.19^{CD}	0.16^{FG}	0.97	5.55
D3	0.87	72.80 ± 3.72	0.17^{DE}	0.18^{EF}	0.98	4.44
D4	0.87	69.30 ± 1.57	0.16^{EF}	0.15^{G}	0.96	3.93
C1	0.77	86.46 ± 2.66	0.14^{GH}	0.27^{C}	0.99	3.01
C2	0.69	82.04 ± 3.28	0.17^{E}	0.22^{D}	0.99	4.44
C3	0.63	74.60 ± 4.51	0.21^{BC}	0.19^{E}	0.99	6.78
C4	0.54	73.60 ± 3.60	0.23^{AB}	0.16^{FG}	0.98	8.13
P-value			<0.0001	<0.0001		
CV(%)			3.52	3.32		
Tukey HSD at 1%			0.0207	0.0262		

a, release rate constant; b, diffusion exponent; R, correlation coefficient; Means with at least one letter common are not statistically significant (1%) using TUKEY's Honest Significant Difference (HSD); CV (%), coefficient of variation.
[a] Boron content (%).
[b] Boron loading efficiency (%).
[c] Diffusion coefficient ($\times 10^{-5}$ mm^2 Day^{-1}).

As the study suggests Fickian behavior of release mechanism, the diffusion coefficient (D_i) of borate from developed composites in water was determined using following equation[48]:

$$k = 4\left[\frac{D_i}{\pi h^2}\right]^{\frac{1}{2}} \quad (10)$$

where, D_i is the diffusion coefficient for the borate ion release and h is the thickness of the loaded sample. Table III shows the D_i values of borate ion form BSAPCs with different reaction parameters.

CONCLUSIONS

The present study concludes synthesis of novel B delivery device where slow release of B was achieved through synthesis of BSAPCs by free radical polymerization technique and it was found that during *in situ* loading, the borax caused highly cross-linked polymer network resulting hydrogel composites with higher mechanical strength. High loading of borax in the developed B formulation has caused reduced water absorbency and enhanced storage modulus (G') of hydrogel composites leading to slower rate of release of B.

REFERENCES

1. Sarkar, D. J.; Singh, A.; Mandal, P.; Kumar, A.; Parmar, B. S. *Polym-Plast. Technol. Eng.* **2015**, *54*, 357.
2. Peng, L.; Zhou, L.; Li, Y.; Pan, F.; Zhang, S. *Compos. Sci. Technol.* **2011**, *71*, 1280.
3. Xu, K.; Wang, J.; Xiang, S.; Chen, Q.; Yue, Y.; Su, X.; Song, C.; Wang, P. *Compos. Sci. Technol.* **2007**, *67*, 3480.
4. Li, A.; Wang, A.; Chen, J. *J. Appl. Polym. Sci.* **2004**, *94*, 1869.
5. Park, H. W.; Lee, W. K.; Park, C. Y.; Cho, W. J. *J. Mater. Sci.* **2003**, *38*, 909.
6. Bhardwaj, A. K.; Shainberg, I.; Goldstein, D.; Warrington, D. N.; Levy, G. *J. Soil. Sci. Soc. Am. J.* **2007**, *71*, 406.
7. Singh, A.; Sarkar, D. J.; Singh, A. K.; Parsad, R.; Kumar, A.; Parmar, B. S. *J. Appl. Polym. Sci.* **2011**, *120*, 1448.
8. Poorna Chandrika, K. S. V.; Singh, A.; Sarkar, D. J.; Rathore, A.; Kumar, A. *J. Appl. Polym. Sci.* **2014**, *131*, 41060.
9. Rudzinski, W. E.; Dave, A. M.; Vaishnav, U. H.; Kumbar, S. G.; Kulkarni, A. R.; Aminabhavi, T. M. *Des Monomers Polym.* **2002**, *5*, 39.
10. Aouada, F. A.; de Moura, M. R.; Orts, W. J.; Mattoso, L. H. C. *J. Mater. Sci.* **2010**, *45*, 4977.
11. Xie, L.; Liu, M.; Ni, B.; Zhang, X.; Wang, Y. *Chem. Eng. J.* **2011**, *167*, 342.
12. Sarkar, S.; Datta, S. C.; Biswas, D. R. *J. Appl. Polym. Sci.* **2014**, *131*, DOI: 10.1002/app.39951.
13. Bortolin, A.; Aouada, F. A.; de Moura, M. R.; Ribeiro, C.; Longo, E.; Mattoso, L. H. C. *J. Appl. Polym. Sci.* **2012**, *123*, 2291.
14. Rudzinski, W. E.; Chipuk, T.; Dave, A. M.; Kumbar, S. G.; Aminabhavi, T. M. *J. Appl. Polym. Sci.* **2003**, *87*, 394.
15. Abat, M.; Degryse, F.; Baird, R.; McLaughlin, M. *J. Soil Sci. Soc. Am. J.* **2015**, *79*, 97.
16. Deb, D. L.; Sakal, R.; Dutta, S.P. In Fundamental of Soil Science; Goswami N. N., Rattan, R. K., Dev, G., Narayanasamy, G., Das, D. K., Sanyal, S.K., Pal, D. K., Rao, D. L. N., Eds.; Indian Society of Soil Science: New Delhi, **2009**; Chapter 20, p 461.
17. Takkar, P. N. *J. Indian Soc. Soil Sci.* **1996**, *44*, 562.
18. Goldbach, H. E.; Huang, L.; Wimmer, M. A. In Advances in Plant and Animal Boron Nutrition; Xu. F., Goldbach. H. E., Brown, P. H., Bell, R. W., Fujiwara, T., Hunt. C. D., Goldberg, S., Shi, L., Eds.; Springer: Online, **2007**; Chapter 1, p 3.
19. Sreedhar, B.; Sairam, M.; Chattopadhyay, D. K.; Rathnam, P. A. S.; Rao, D. V. M. *J. Appl. Polym. Sci.* **2005**, *96*, 1313.
20. Coviello, T.; Matricardi, P.; Balena, A.; Chiapperino, B.; Alhaique, F. *J. Appl. Polym. Sci.* **2010**, *115*, 3610.
21. Lai, C. L.; Chen, J. T.; Fu, Y. J.; Liu, W. R.; Zhong, Y. R.; Huang, S. H.; Hung, W. S.; Lue, S. J.; Hu, C. C.; Lee, K. R. *Carbon* **2015**, *82*, 513.
22. Cheng, Q.; Jiang, L.; Tang, Z. *Acc. Chem. Res.* **2014**, *47*, 1256.
23. Benli, B. *J. Appl. Polym. Sci.* **2013**, *128*, 4172.
24. Natali, I.; Carretti, E.; Angelova, L.; Baglioni, P.; Weiss, R. G.; Dei, L. *Langmuir* **2011**, *27*, 13226.
25. Wang, J.; Lin, L.; Cheng, Q.; Jiang, L. *Angew. Chem. Int. Ed.* **2012**, *51*, 4676.
26. Gong, J. P.; Katsuyama, Y.; Kurokawa, T.; Osada, Y. *Adv. Mater.* **2003**, 1155. 15
27. Sun, T. L.; Kurokawa, T.; Kuroda, S.; Ihsan, A. B.; Akasaki, T.; Sato, K.; Haque, M. A.; Nakajima, T.; Gong, J. P. *Nat. Mater.* **2014**, *12*, 932.
28. Kamata, H.; Akagi, Y.; Kayasuga-Kariya, Y.; Chung, U.; Sakai, T. *Science* **2014**, *343*, 873.
29. Pathania, D.; Sharma, R. *Adv. Mat. Lett.* **2012**, *3*, 136.
30. Guo, W. Y.; Peng, B. *J. Vinyl Addit. Technol.* **2012**, *18*, 261.
31. Sommers, L. E.; Nelson, D. W. *Soil Sci. So. Am. J.* **1972**, *36*, 902.
32. John, M. K.; Chuah, H. H.; Neufeld, J. H. *Anal. Lett.* **1975**, *8*, 559.
33. Ritger, P. L.; Peppas, N. A. *J. Control. Release* **1987**, *5*, 23.
34. Wang, W.; Chen, K.; Zhang, Z. *J. Phys. Chem. C* **2009**, *113*, 2699.
35. Gumus, O. Y.; Unal, H. I.; Erol, O.; Sari, B. *Polym. Compos.* **2011**, *32*, 418.
36. Younes, H. M.; Bravo-Grimaldo, E.; Amsden, B. G. *Biomaterials* **2004**, *25*, 5261.
37. Chen, L.; Ahadi, A.; Zhou, J.; Ståhl, J. E. *Proc. CIRP* **2013**, *8*, 334.
38. MohyEldin, M. S.; Omer, A. M.; Soliman, E. A.; Hassan, E. A. *Desalin. Water Treat.* **2013**, *51*, 3196.
39. Moreiraa, H. R.; Munarinb, F.; Gentilini, R.; Visai, L.; Granjaa, P. L.; Tanzi, M. C.; Petrini, P. *Carbohydr. Polym.* **2014**, *103*, 339.
40. Saini, D. R.; Shenoy, A. V. *Polym. Eng. Sci.* **1986**, *26*, 441.

41. Shenoy, A. V. In Rheology of Filled Polymer Systems; Springer: Netherland, **1999**; Chapter 2, p 90.
42. Ramkumar, D. H. S.; Bhattacharya, M.; Menjivar, J. A.; Huang, T. A. *J. Texture Stud.* **1996**, *27*, 517.
43. Grassi, M.; Lapasin, R.; Coviello, T.; Matricardi, P.; Meo, C. D.; Alhaique, F. *Carbohydr. Polym.* **2009**, *78*, 377.
44. Jianga, H.; Sua, W.; Mathera, P. T.; Bunninga, T. J. *Polymer* **1999**, *40*, 4593.
45. Zhou, W. J.; Yao, K. J.; Kurth, M. J. *J. Appl. Polym. Sci.* **1996**, *62*, 911.
46. Yang, J.; Zhao, J. J.; Han, C. R.; Duan, J. F. *Compos. Sci. Technol.* **2014**, *95*, 1.
47. Dini, E.; Alexandridou, S.; Kiparissides, C. *J. Microencapsul.* **2003**, *20*, 375.
48. Mullarney, M. P.; Seery, T. A. P.; Weiss, R. A. *Polymer* **2006**, *47*, 3845.